

New applications of Renormalization Group methods to nuclear matter

Kai Hebeler

Department of Physics, The Ohio State University, Columbus, OH 43210, USA

Abstract. We give an overview of recent results for the nuclear equation of state and properties of neutron stars based on microscopic two- and three-nucleon interactions derived within chiral effective field theory (EFT). It is demonstrated that the application of Renormalization Group (RG) transformations allows efficient, controlled and simplified calculations of nuclear matter.

Keywords: Nuclear equation of state, Three-nucleon forces, Neutron stars, Renormalization Group

PACS: 26.60.-c, 21.65.Cd, 05.10.Cc, 97.60.Jd

THE SIMILARITY RENORMALIZATION GROUP

Establishing an interparticle Hamiltonian, which is the fundamental ingredient for microscopic many-body calculations of atomic nuclei and nucleonic matter, is a difficult and on-going challenge for low-energy nuclear physics. Chiral EFT and RG methods make feasible a controlled description of nuclear interactions, grounded in QCD symmetries, which in turn makes possible the description of nuclei across the nuclear many-body landscape [1, 2]. The two-body sector has been solved in the sense that various nucleon-nucleon interactions are available that reproduce low-energy scattering phase shifts to high accuracy. The unsettled frontier is three- and higher-body forces, which play a key role in many-nucleon systems.

Nuclear structure calculations are complicated due to the coupling of low to high momenta by nuclear interactions. A fruitful path to decoupling high-momentum from low-momentum physics is the Similarity Renormalization Group (SRG), which is based on a continuous sequence of unitary transformations that suppress off-diagonal matrix elements. The decoupling of momenta via the SRG has been demonstrated for nuclear nucleon-nucleon (NN) interactions [3] and very recently for the first time also for three-nucleon forces (3NF) [4]. The decoupling in 3NF is illustrated in Fig. 1: at large resolution scales $\lambda = \infty$ the potential contains significant off-diagonal couplings. As we evolve to lower resolution, these couplings get successively suppressed and finally at $\lambda = 1.5 \text{ fm}^{-1}$ the non-perturbative features are substantially softened as we find only non-vanishing strength at small momenta and around the diagonal.

SRG-evolved potentials are automatically energy independent and the same transformations renormalize all operators, including many-body operators, and the class of transformations can be tailored for effectiveness in particular problems. When evolving nuclear interactions to lower resolution, it is inevitable that many-body interactions and operators are induced even if initially absent. This might be considered as unnatural if nuclei could be accurately calculated based on only NN interactions, as was assumed

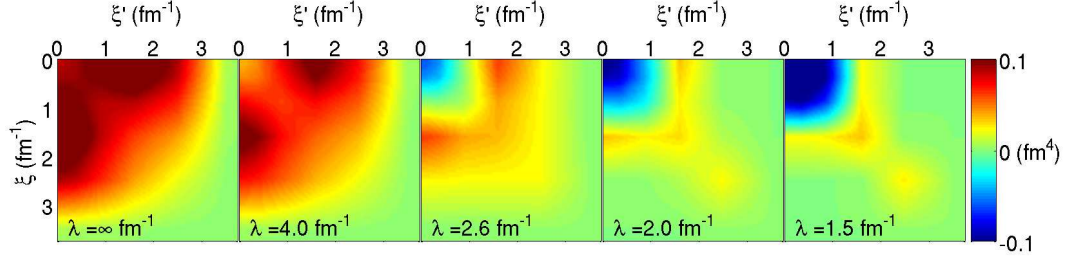


FIGURE 1. (from Ref. [4]) Contour plot of the RG-evolved 3N potential as a function of the hypermomenta ξ and ξ' for a fixed hyperangle. Evolution proceeds from left to right, with softening evidence by the suppression of off-diagonal elements.

for much of the history of nuclear structure calculations. However, chiral EFT reveals the natural scale and hierarchy of many-body forces, which dictates their inclusion in modern calculations of nuclei and nucleonic matter.

NUCLEAR EQUATION OF STATE

Progress towards controlled nuclear matter calculations has long been hindered by the non-perturbative nature of the nuclear many-body problem when conventional nuclear potentials are used. The novel developments described above open new ways to overcome these obstacles. Calculations of finite nuclei based on consistently evolved NN and 3N potentials are now available (see Refs. [5]). Such fully consistent calculations of the nuclear equation of state do not easily follow, but the framework recently presented in Ref. [4] makes them likely in the near future.

As an alternative simplified strategy it is also possible to evolve only the NN interactions with RG methods and then fix the short-range parameters of the 3N forces from fits to few-body systems at the low-momentum scale [6]. This procedure assumes that the long-range part of the 3N forces remains invariant under the RG transformations and that the operator structure of the chiral interaction is a sufficiently complete basis so that induced contributions can be absorbed to good approximation. As shown in the left panel of Fig. 2, we find realistic saturation properties within our theoretical uncertainty bounds without adjustment of free parameters. The two pairs of curves show the difference between the nuclear matter results for NN-only and NN plus 3N interactions. It is evident that saturation is driven by 3NF. Even for $\Lambda = 2.8 \text{ fm}^{-1}$, which is similar to the lower cutoffs in chiral EFT potentials, saturation is at too high density without the 3NF.

Neutron matter provides a different perspective to nucleonic matter. Here only the long-range 2π -exchange 3NF contribute [7], which implies that all three- and four-neutron (4N) forces are predicted up to $N^3\text{LO}$. The physics of neutron matter ranges from the universal regime at low densities that can be probed in experiments with ultracold atoms up to high densities relevant for the structure of neutron stars. For these extreme conditions, controlled calculations with theoretical error estimates are essential. As a result of effective range effects, restricted phase space at finite density and weaker tensor forces between neutrons neutron matter behaves more perturbative

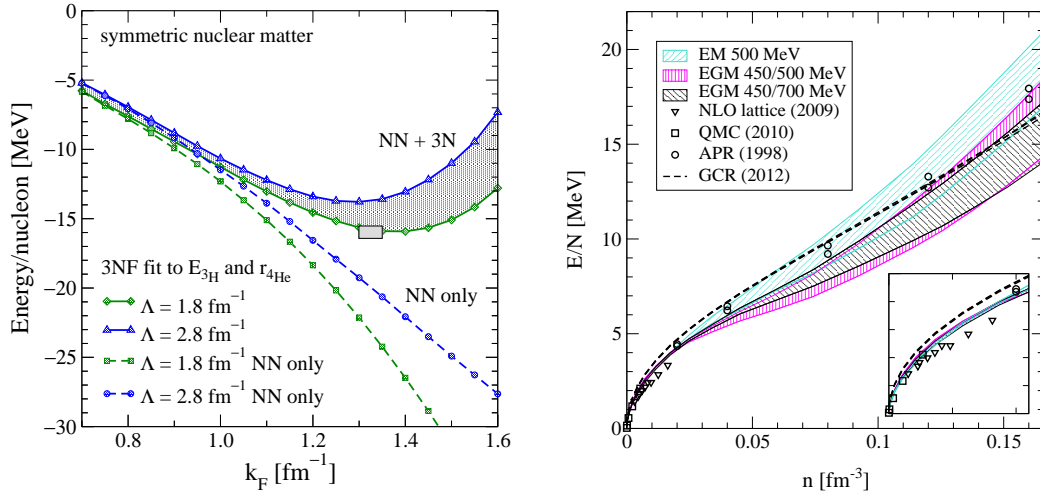


FIGURE 2. left panel: (from Ref. [6]) Nuclear matter energy as a function of the Fermi momentum based on NN+3NF forces compared to NN-only results for two representative NN cutoffs and a fixed 3N cutoff; right panel: (from Ref.[8]) Neutron matter energy as a function of density including NN, 3N and 4N forces up to N^3 LO in comparison to other studies.

than symmetric nuclear matter. In the right panel of Fig. 2 we present results for neutron matter based directly on chiral EFT interactions without RG evolution including all NN, 3N and 4N contributions up to N^3 LO [8]. We find relatively large attractive contributions from N^3 LO 3N forces, which might be an indication that a chiral EFT with explicit Δ degrees of freedom may be more efficient [1]. In contrast, contributions from 4N interactions appear to be very small in neutron matter.

ASTROPHYSICAL APPLICATIONS

Core densities inside a neutron star can reach several times nuclear saturation density. For this reason, we need to extend the microscopically calculated EOSs to higher densities. To do so we use a general strategy which does not rely on assumptions about the nature of the constituents of the matter and their interactions at higher densities: we employ a piecewise polytropic ansatz $P(\rho) = \kappa \rho^\Gamma$ [9] (see also Refs. [10, 11]), whereas the values of the parameters are limited by physics and constraints from observations. As constraints we require that (a) the speed of sound remains smaller than the speed of light for all densities, and (b) the EOS is able to support a neutron star of mass $M \geq M_{\min}$, where the value of M_{\min} is given by experimental neutron star observations. For M_{\min} we consider two cases: first, $M_{\min} = 1.97 M_\odot$, which is currently the heaviest confirmed observed neutron star mass [12], and second, a hypothetical mass $M_{\min} = 2.4 M_\odot$. We generate a very large number of EOSs for different values of parameters and retain only those which fulfill the causality and mass conditions. This results in uncertainty bands for the pressure and neutron star radii, which are shown in Fig. 3. In the left panel we present the uncertainty bands for the equation of state for the two mass constraints compared to a representative set of other EOSs (see Ref. [13]). We find that only a

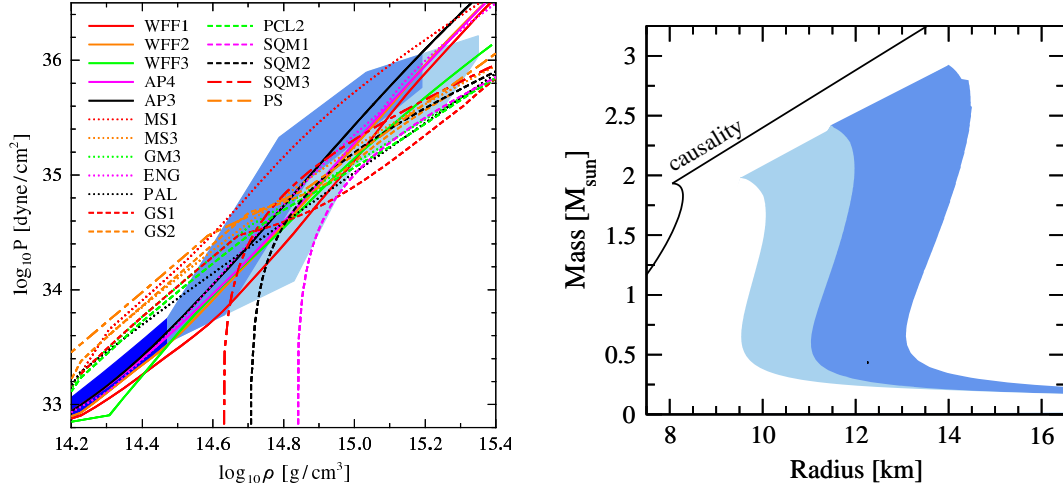


FIGURE 3. left panel: uncertainty of the pressure as a function of mass density compared to a representative set of equations of state used in the literature (see Ref. [13]); right panel: corresponding uncertainty of neutron star radius and mass. For both panels, the light band corresponds to the mass constraint $M_{\text{min}} = 1.97 M_{\odot}$ and the dark band to $M_{\text{min}} = 2.4 M_{\odot}$. See Ref. [9] for details.

relatively small number of EOSs are compatible with the extracted uncertainty bands for all densities. In the right panel we show the resulting constraints for the radius of neutron stars. For a typical neutron star of mass $M = 1.4 M_{\odot}$ we find a radius range $R = 10.0 - 13.7$ km for $M_{\text{min}} = 1.97 M_{\odot}$ and $R = 11.6 - 13.7$ km for $M_{\text{min}} = 2.4 M_{\odot}$.

CORRELATIONS IN NUCLEAR SYSTEMS

Recent experimental studies of proton knock-out reactions off nuclei at high-momentum transfer have been explained by invoking short-range correlations (SRC) in nuclear systems [14]. Such explanations may seem at odds with RG evolution, which leads to many-body wave functions with highly suppressed SRC. The key is that not only the Hamiltonian but every other operator must also evolve. Recent advances make it possible to systematically evolve operators using the SRG as shown in Ref. [15].

In Fig. 4 we show first preliminary results for the pair momentum distribution $\rho(P, q)$ in nuclear matter as a function of the relative momentum q , obtained within a perturbative expansion [16]. Here P denotes the center-of-mass momentum of the pair. We choose as initial Hamiltonian the highly non-perturbative Argonne V18 NN potential and evolve consistently density operator and Hamiltonian via the SRG, each truncated at the two-body level. As shown in the left panel, already at this level of approximation, the pair momentum distribution function is invariant to good approximation in back-to-back kinematics, in contrast to the case without operator evolution (dotted lines). In addition, we are also able to reproduce the enhancement of neutron-proton pairs over neutron-neutron pairs due to the tensor interaction of the initial Hamiltonian (see right panel). Furthermore, in the present kinematic conditions there is factorization of the unitary transformation, which leads to significant simplifications and an alternative in-

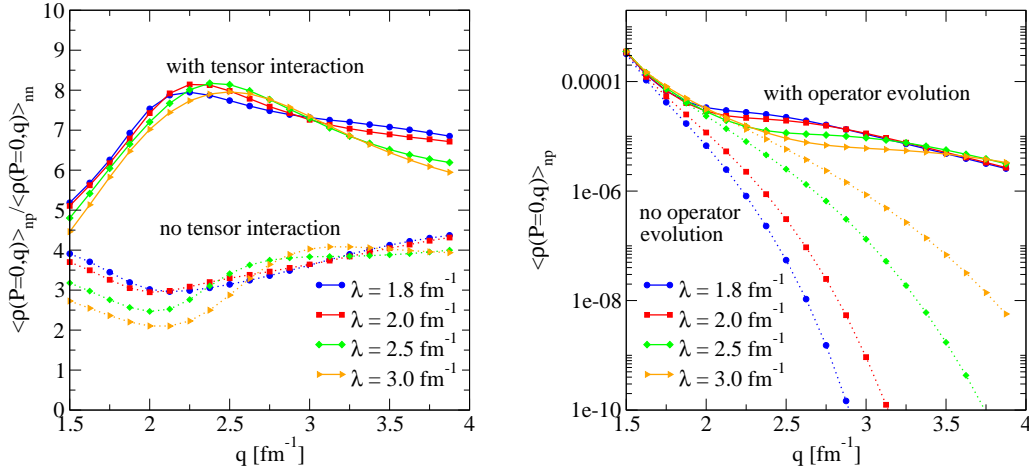


FIGURE 4. The pair density function in nuclear matter at saturation density as a function of relative momentum q for different SRG resolution scales λ . The left panel demonstrates the importance of a consistent evolution of Hamiltonian and density operator, the right panel the significance of tensor forces in the initial Hamiltonian, leading to an enhancement of neutron-proton pairs over neutron-neutron pairs.

terpretation of the universal high-momentum dependence and scaling [15]. This also illustrates that physical interpretations and intuition in general depend on the resolution, whereas the RG is the tool that allows us to connect the different pictures.

ACKNOWLEDGMENTS

I would like to thank R. J. Furnstahl for helpful comments on the manuscript. This work was supported by the NSF under Grant No. PHY-1002478.

REFERENCES

1. E. Epelbaum, H.-W. Hammer and U.-G. Meissner, Rev. Mod. Phys. **81**, 1773 (2009).
2. S. K. Bogner, R. J. Furnstahl and A. Schwenk, Prog. Part. Nucl. Phys. **65**, 94 (2010).
3. S. K. Bogner, R. J. Furnstahl and R. J. Perry, Phys. Rev. C **75**, 061001(R) (2007).
4. K. Hebeler, Phys. Rev. C **85**, 021002(R) (2012).
5. E. D. Jurgenson, P. Navratil and R. J. Furnstahl, Phys. Rev. Lett. **103**, 082501 (2009), E. D. Jurgenson, P. Navratil and R. J. Furnstahl, Phys. Rev. C **83**, 034301, (2011), R. Roth *et al.*, Phys. Rev. Lett. **107**, 072501 (2011).
6. K. Hebeler *et al.*, Phys. Rev. C **83**, 031301(R) (2011).
7. K. Hebeler and A. Schwenk, Phys. Rev. C **82**, 014314 (2010).
8. I. Tews, T. Krueger, K. Hebeler and A. Schwenk, arXiv: 1206.0025
9. K. Hebeler, J. M. Lattimer, C. J. Pethick and A. Schwenk, in preparation.
10. J. S. Read, B. D. Lackey, B. J. Owen, and J. L. Friedman, Phys. Rev. D **79**, 124032 (2009).
11. K. Hebeler, J. M. Lattimer, C. J. Pethick and A. Schwenk, Phys. Rev. Lett. **105**, 161102 (2010).
12. P. B. Demorest *et al.*, Nature **467**, 1081 (2010).
13. J. M. Lattimer and M. Prakash, Astrophys. J. **550**, 426 (2001).
14. R. Subedi *et al.*, Science **320**, 1476 (2008).
15. E. R. Anderson, S.K. Bogner, R.J. Furnstahl and R.J. Perry, Phys. Rev. C **82**, 054001 (2010).
16. E. R. Anderson, R. J. Furnstahl and K. Hebeler, in preparation.